Supporting information

Black-to-Transparent Electrochromic Capacitive Windows Based on Conjugated Polymers

*Minsu Han,† Cheolhyon Cho,† Hwandong Jang, and Eunkyoung Kim**

Department of Chemical and Biomolecular Engineering, Yonsei University, 50 Yonsei-ro, Seodaemun-gu, Seoul 03722, South Korea, E-mail: eunkim@yonsei.kr

Corresponding Author

*E-mail: eunkim@yonsei.ac.kr.

†These authors contributed equally to this work

Supporting Information includes:

S1. Supporting experimental section

S2. Supporting Figure

S3. Supporting Table

S4. Supplementary Video

S1. Supporting Experimental section

S1.1. Instrument.

The electrochemical properties were measured by the universal potentiostat [model CHI 624B (CH Instruments, Inc.). Optical properties were obtained by a PerkinElmer Lambda 750 UV/vis/NIR spectrophotometer. Scanning electron microscopy (SEM) was performed using a JEOLJSM-7001F. Thickness was obtained using a Bruker Surface Profiler (DektakXT). Gel permeation chromatography (GPC) was performed using an YL9100 GPC System with its internal differential refractive index detector at 25 °C. Retention times were calibrated against narrow molecular weight polystyrene standards (Standard SM-105, Shodex). The structure of the material was analyzed by 300MHz ^{1}H NMR (Bruker biospin AVANCE III HD 300). The crystal structures of the samples were determined by X-Ray Diffraction Analyzer (Ultima IV). Raman spectra were obtained using a Laser Raman spectroscopy (LabRAM Aramis, HORIBA) using a 532 nm ion laser. XPS data was analyzed by K-alpha. Surface area was analyzed by Autosorb-iQ 2ST/MP (BET).

S1.2. Synthesis of black ECPs

Synthesis of 3,3-bis(bromomethyl)-3,4-dihydro-2H-thieno[3,4-b][1,4]dioxepine (1)

3,4-dimethoxythiophene (10 g, 69.4 mmol), 2,2-bis(bromomethyl)propane-1,3-diol (36 g, 138.8 mmol), p-toluenesulfonic acid (1.2 g, 6.94 mmol) were added to a 500 mL three-neck round bottom flask. After being degassed during 30 minutes and refilled with argon, toluene 300 mL was added. The reaction mixture was stirred at 120 ℃ during overnight and washed with DI water. After removing solvent, the crude products were purified by column chromatography with hexane and methylene chloride as an eluent (hexane: MC = 4:1) to give

a white solid.

3,3-bis((2-ethylhexyloxy)methyl)-3,4-dihydro-2H-thieno[3,4-b][1,4]dioxepine (EH)

60% NaH (1.35 g, 3 eq) and a stirring bar were added into 250 ml 3-neck round bottom flask connected with the reflux condenser and dropping funnel. After being degassed during 1 hr, Argon gas was refilled and anhydrous hexane 15 ml was added. After increasing temperature to 40 ℃, 2-ehtylhexan-1-ol 2.21 g and anhydrous DMF 30 ml were added into the dropping funnel. Color changed from white to yellow as 2-ehtylhexan-1-ol reacted with NaH. After dropping them, temperature was increased to 70 ℃ and the reaction mixture was stirred during 6 hr. After 6 hr, compound 1 1g was added. After 2 days, the reaction mixture was washed with DI water and hexane. After removing solvents, the crude products were purified by column chromatography with hexane and methylene chloride as an eluent (hexane: mc = 1:1) to give a colorless oil.

Synthesis of 3,3-bis((2-ethylhexyloxy)methyl)-6,8-dibromo-3,4-dihydro-2H-thieno[3,4-b][1,4] dioxepine (2,5-dibromoEH)

EH (1 g, 2.3 mmol), N-bromosuccinimide (1 g, 5.6 mmol), DMF 12.5 ml were added to 50ml 2-neck round bottom flask. The reaction mixture was stirred at room temperature during 30 minutes. It was diluted by ethyl acetate and washed with water 200 mL 2 times. After evaporating solvent, the crude product was purified with hexane by column chromatography to give white solid (1.48 g, 91.7 %).

General procedure for polymerization of ECP

EH (1.1 g, 2.5 mmol), 2,5-dibromoEH (1.12 g, 1.87 mmol), BT (0.18 g, 0.62 mmol), pivalic acid (0.16 g, 1.55 mmol), K_2CO_3 (1.77 g, 12.8 mmol), 5% palladium(II) acetate (0.028 g, 0.12 mmol) and DMAc 30 ml were added into round bottom flask. The reaction mixture was stirred at 150 ℃ during 24 hrs. After 24 hr, the mixture was cooled to room temperature and the solution was poured into methanol to give a precipitate. The precipitate was 3 times filtered with methanol, hexane and acetone, respectively. The obtained polymer PEB1 was a black solid (1.01 g, 42 %). Other polymers PEB0 and PEB2 were synthesized by varying the molar ratio. PEB0 was a purple solid (0.93 g, 52 %), and PEB2 was a blue solid (1.46 g, 71 %).

PEB0 ^{1}H NMR (300 MHz, $CDCl_3$) δ 4.39-4.00 (m, 4H), 3.60 (bs, 4H), 3.33 (bs,4H), 1.45-1.05 (m, 18H), 0.89 (bs, 12H)

PEB1 ^{1}H NMR (300 MHz, $CDCl_3$) δ 8.39-8.25 (m, 2H), 4.39-4.00 (m, 28H), 3.62 (bs, 28H), 3.33 (bs,28H), 1.45-1.10 (m, 126H), 0.89 (bs, 84H)

PEB2 ^{1}H NMR (300 MHz, $CDCl_3$) δ 8.65-8.30 (m, 6H), 4.45-4.06 (m, 20H), 3.67 (bs, 20H), 3.37 (bs,20H), 1.50-1.15 (m, 90H), 0.92 (bs, 60H)

S1.3. Calculation of capacitive properties

In pseudocapacitor type device, the specific capacitance (C_{sp}, F/g), the energy density (E, Wh/kg), and the power density (P, kW/kg) could be calculated from galvanostatic CD curves by using the following equations.[1, 2]

$$C_{sp} = \frac{4I}{mdV/dt}$$

$$E = \frac{C_{sp}V^2}{8}$$

$$P = \frac{E}{dt}$$

where I is the current at charging and discharging process, m is the mass loading of the active material, dV is the voltage drop upon discharging, and dt is the total discharging time. The total mass of the polymers corresponding to redox-active substances in ECCW100 was 0.0315 mg.

S2. Supporting Figure S1~S13

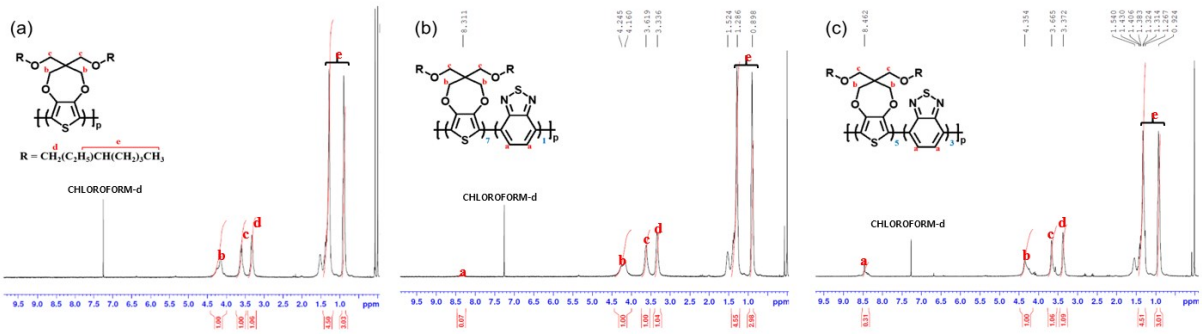

Supporting Figure 1. a-c) ^{1}H NMR spectra of ECP (a) PEB0, (b) PEB1, and (c) PEB2 in $CDCl_3$.

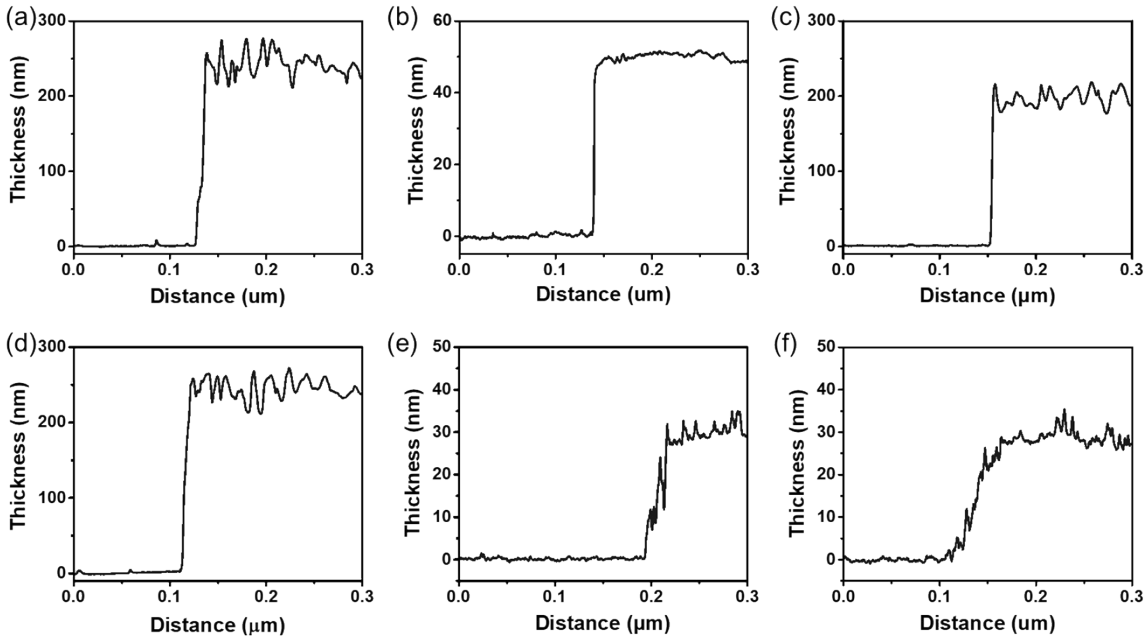

Supporting Figure 2. Surface profile of a) PEB1 film (250 nm), b) PR-Br film (50 nm), c) PEB1 film (200 nm), d) PEB1PR film (250 nm), e) PGF0 film, and f) PGF100 film.

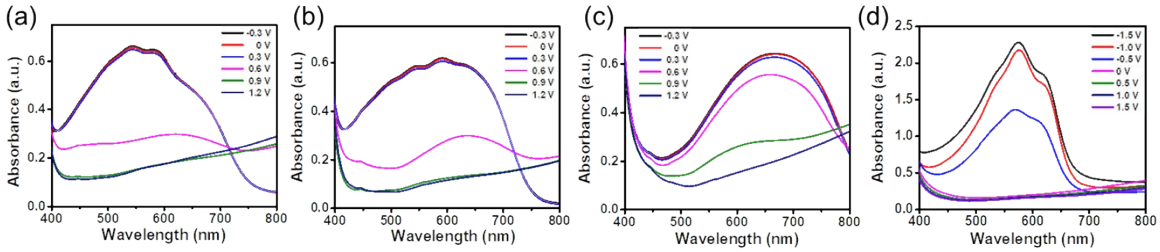

Supporting Figure 3. In-situ spectrochemistry of (a) PEB0 film, (b) PEB1 film, (c) PEB2 film, and (d) PR-Br film on ITO glass. The thickness of the films was 250 nm.

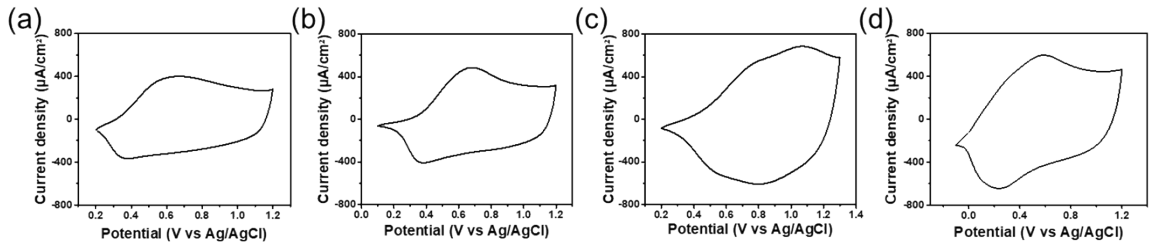

Supporting Figure 4. Cyclic voltammogram at a scan rate of 100 mV s^{-1} (vs. Ag/AgCl) for (a) PEB0 film, (b) PEB1 film, (c) PEB2 film, and (d) PR-Br film on ITO glass. The thickness of the films was 250 nm.

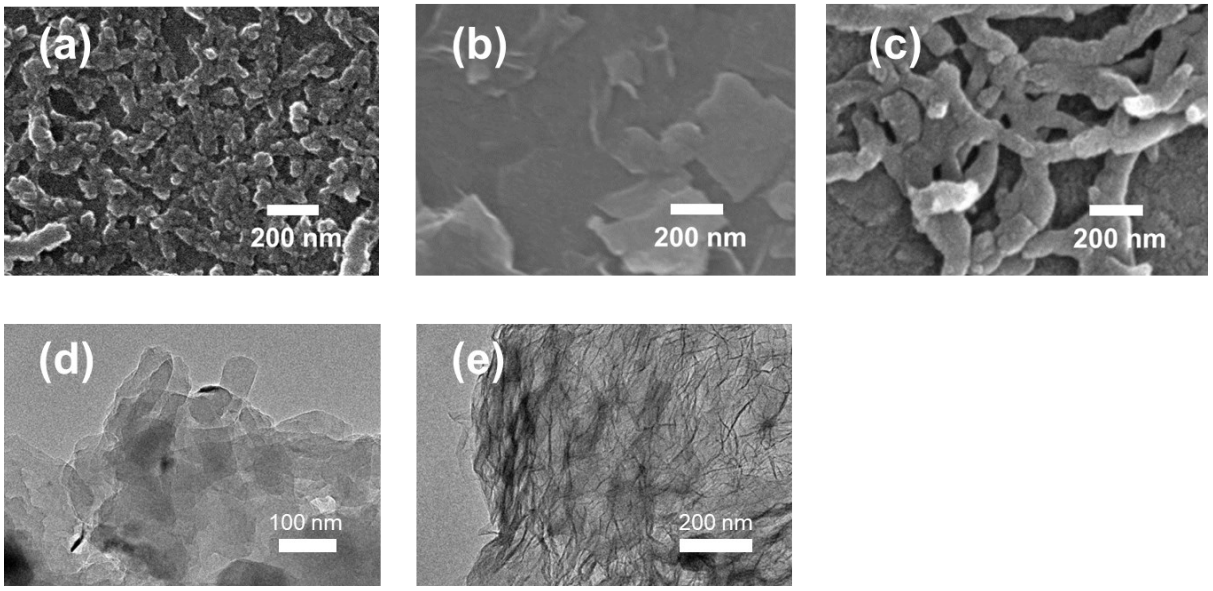

Supporting Figure 5. a-c) SEM images of (a) PGF0, (b) pure GF, and (c) PANI^{E}. d and e) TEM images of (d) PGF0 and (e) pure GF.

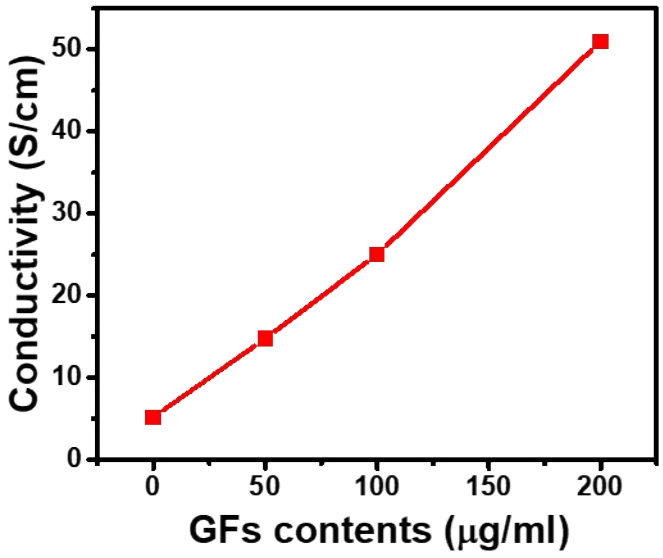

	PGF0	PGF50	PGF100	PGF200
Conductivity (S cm^{-1})	5.18	14.8	25.0	51.0

Supporting Figure 6. Electrical conductivity of PGF according to the amount of GF added when synthesizing PANI (top). Specific values are listed in the table (bottom).

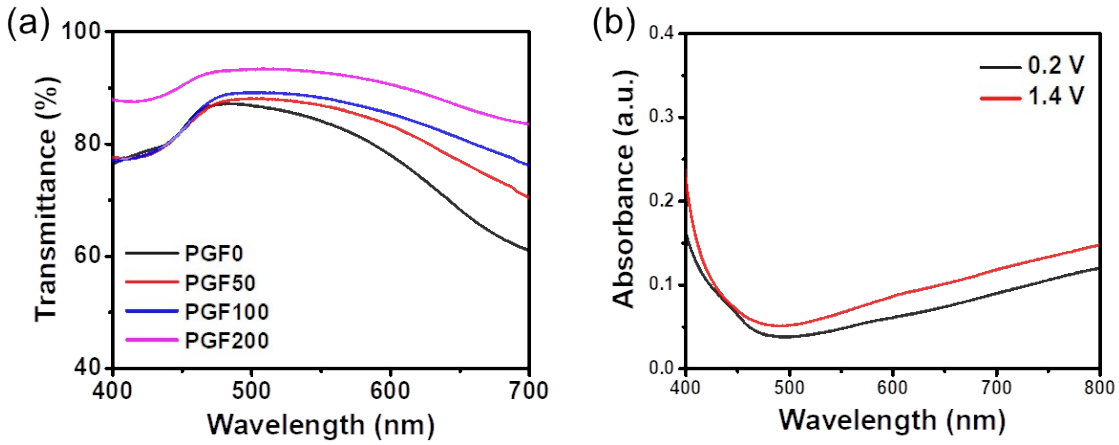

Supporting Figure 7. a) Transmittance of PGF. The films were soaked in SPAn and measured in doped state. The thickness of the films is 30 nm. b) In-situ spectroelectrochemistry of PGF100. The electrochemical redox of PGF100 was performed using Ag/AgCl electrode as the RE, stainless steel as the CE, and SPAn as the electrolyte.

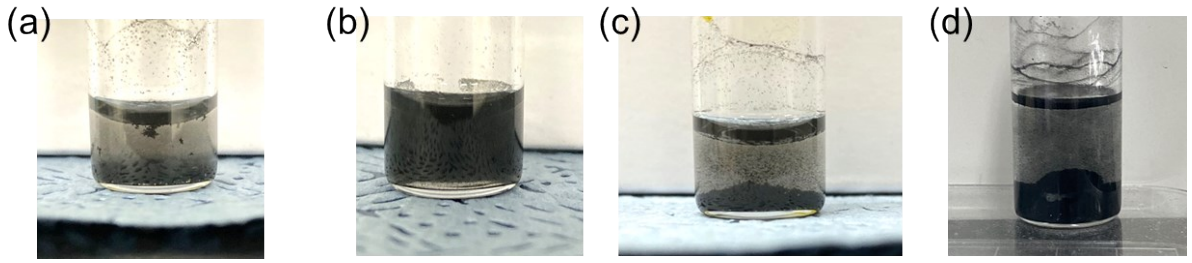

Supporting Figure 8. a and b) Photographs of GFs solution (100 µg/ml) dispersed by ultrasonication (a) in 1 M HCl solution and (b) in 0.25 M aniline solution (in 1 M HCl solution). c) Photograph of GF solution (200 µg/ml) dispersed by ultrasonication in 0.25 M aniline solution (in 1 M HCl solution). d) Photograph of GF solution (100 µg/ml) dispersed by mechanically stirring in 0.25 M aniline solution (in 1 M HCl solution).

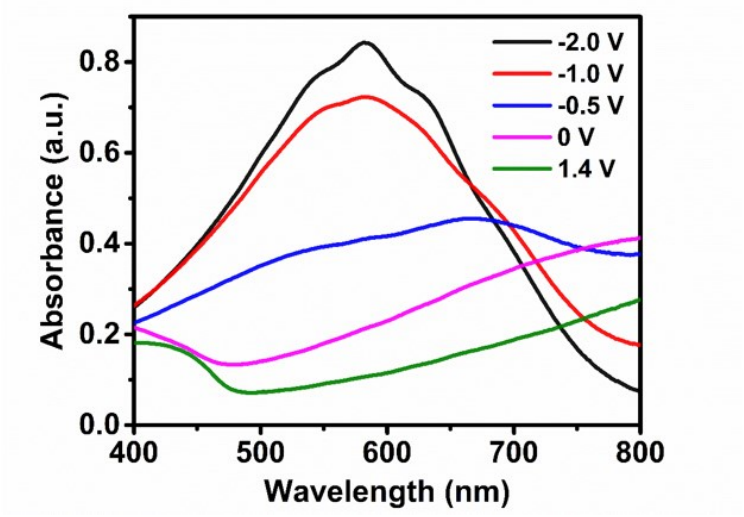

Supporting Figure 9. In-situ spectrochemistry of the ECCW100 with PEB1PR (250 nm) and PGF100 (30 nm).

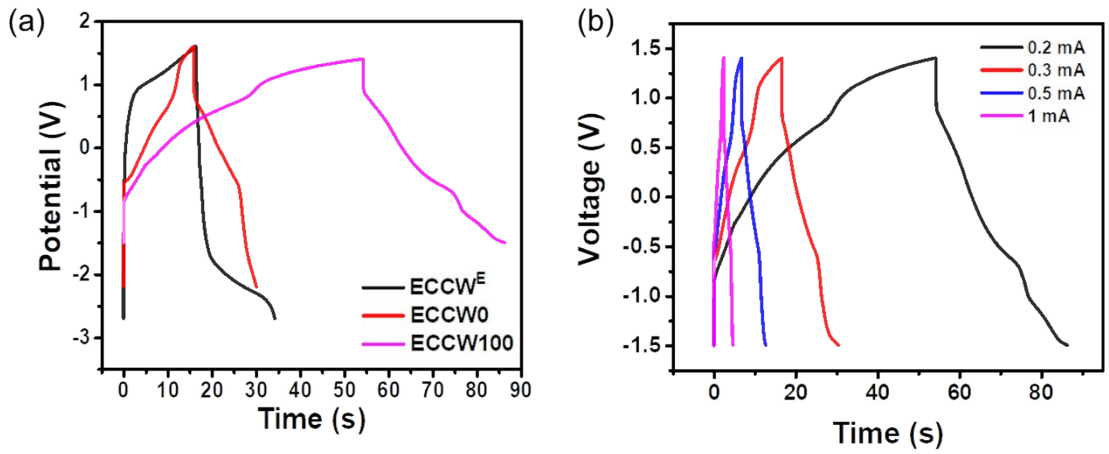

Supporting Figure 10. a) Galvanostatic CD curves of $ECCW^E$ (black), ECCW0 (red), and ECCW100 (magenta) in different potential windows. $ECCW^E$: 1.6/-2.7 V, ECCW0: 1.6/-2.2 V, and ECCW100: 1.4/-1.5 V. b) Galvanostatic CD curves of ECCW100 within a potential window of 1.4/-1.5 V at different current densities of 0.2, 0.3, 0.5, and 1.0 mA cm^{-2}.

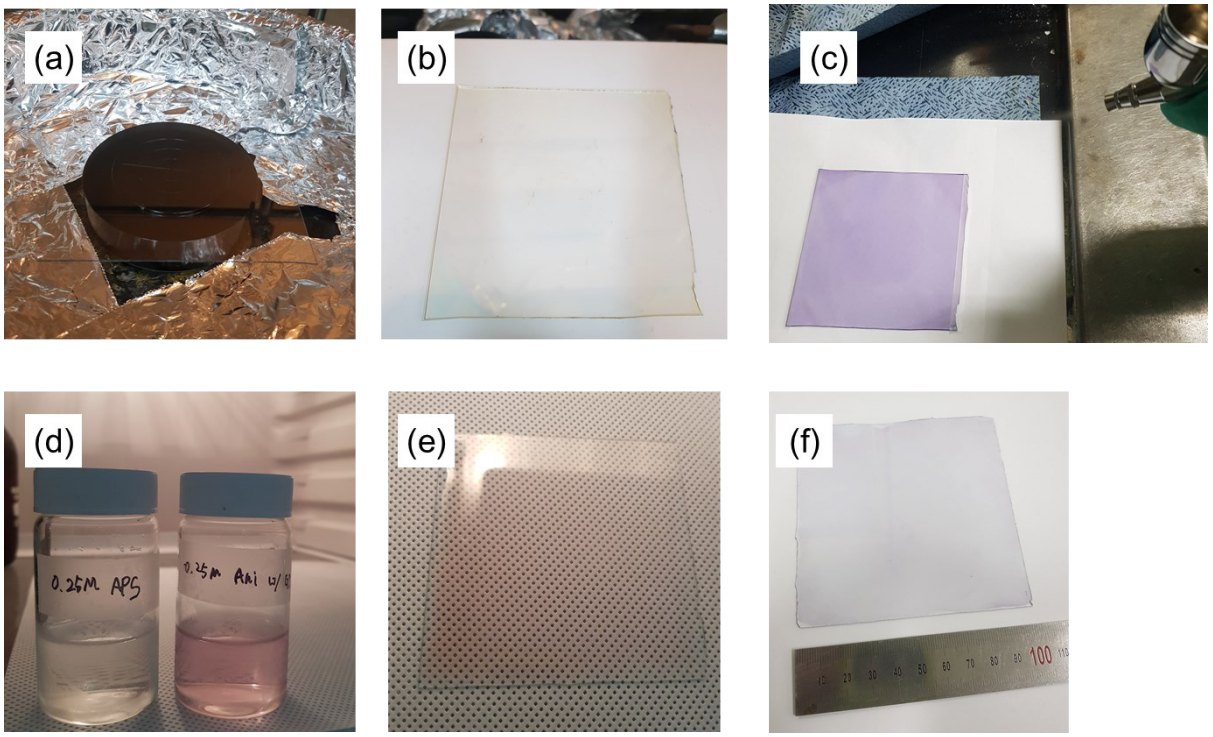

Supporting Figure 11. Photographic images of the detailed process for the preparation of the large area ECCW100. a) ITO glass fixed on a large chuck, b) ITO glass coated with an oxidant solution containing monomer, c) Spray coating on PR-Br film, d) 0.25 M aniline solution with GFs and 0.25 M APS solution stored at 0°C, e) The mixed solution (APS + Aniline) on the ITO glass, f) PGF100 film after washing.

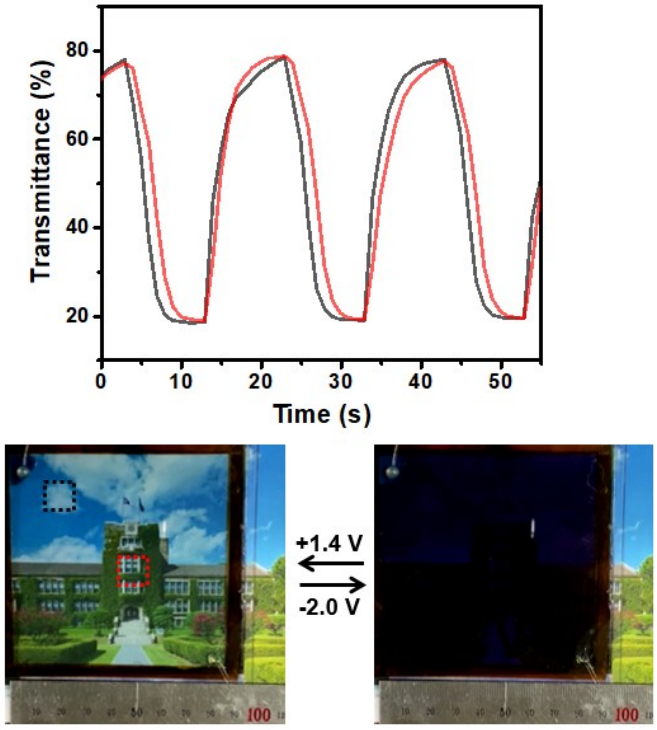

Supporting Figure 12. Transmittance change of the 100 cm^2 ECCW100 in 580 nm at alternate step potentials (1.4 V/-2.0 V). The step potentials were applied at interval of 10 s. The dotted squares with an area of 1 cm^2 were measured, respectively.

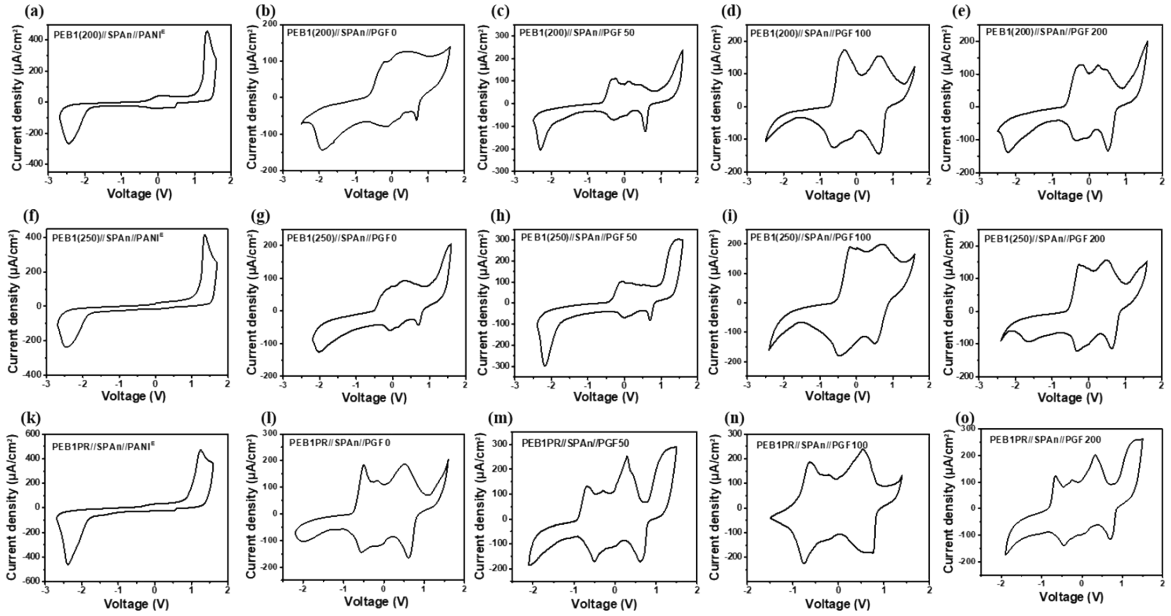

Supporting Figure 13. Cyclic voltammogram of (a~e) PEB1 (T: 200 nm), (f~j) PEB1 (T: 250 nm) and (k~m) PEB1PR (T : 250 nm) with different capacitive layer condition.

S3. Supporting Tables

Supporting Table 1. Molecular weights and PDI measured via GPC.

	EH (1)	**2,5-dibromoEH (x)**	**BT (y)**	**M_n (g/mol)**	**M_w (g/mol)**	**PDI**
PEB0	1	1	0	7,732	9,631	1.2
PEB1	1	0.75	0.25	14,443	21,909	1.5
PEB2	1	0.25	0.75	7,913	10,229	1.3

Supporting Table 2. Capacitive properties of PANI films.

	Applied potential (V/V)	Capacitance[a] (mF cm^{-2} (F g^{-1}))	E_{ox}[b] Peaks (V)	E_{red}[c] Peaks (V)	Onset potential (Ox/Red) (V/V)	Reference
PANI[E]	0/1.4	1.3 (650)	0.37, 1.11	0.49, 1.12	0.33/0.97	This work
PGF0	0/1.4	1.7 (377.8)	0.35, 1.15	0.43, 1.14	0.34/1.01	This work
PGF50	0/1.4	2.4 (533.3)	0.33, 1.14	0.48, 1.14	0.29/0.95	This work
PGF100	0/1.4	2.9 (644.4)	0.31, 1.13	0.51, 1.15	0.28/0.98	This work
PGF200	0/1.4	2.7 (600)	0.32, 1.11	0.44, 1.15	0.28/0.92	This work
GS-PANI	-0.2/1.0	(413.2)[d]	0.34, 0.90	0.10, 0.69	0.21/0.85[e]	3
GNS/PANI	-0.7/0.3	(570)[e]	-0.09[e]	-0.38[e]	-0.36/-0.1[e]	4
RGO/PANI	-0.2/1.0	(732)[f]	0.30, 0.55[c]	0.35, 0.62[e]	0.15/0.75[e]	5
$Ti_3C_2T_x$/PANI	-0.7/0.2	403.7 (301.8)	-0.1[e]	-0.45[e]	-0.32/-0.15[e]	6

[a]Capacitance measured by cyclic voltammetry. All the measurements were done at a scan rate of 100 mV/s unless otherwise noted. [b]Peak oxidation potential. [c]Peak reduction potential. [d]This measurement was done at a scan rate of 110 mV/s. [e]The values inferred from the graph. [f]This measurement was done at a scan rate of 1.4 A/g.

Supporting Table 3. Energy density and power density of ECCW100 according to the different current density.

Current density ($mA\ cm^{-2}$)	**Energy density ($W\ h\ kg^{-1}$)**	**Power density ($kW\ kg^{-1}$)**
0.2	26.9	23.9
0.3	19.4	24.5
0.5	16.5	29.4
1.0	12.4	42.04

Supporting Table 4. EC and capacitive properties of ECCWs under various conditions.

WE (nm)	CE	Capacitance[a] ((mF cm^{-2} (F g^{-1}))	Energy density (W h kg^{-1})	Power density (kW kg^{-1})	Δ%T (%)
PEB1(200)	$PANI^E$	0.09 (3.44)	1.1	8.3	43
PEB1(200)	PGF0	0.59 (30.3)	9.7	24.1	42
PEB1(200)	PGF50	0.91 (46.6)	14.9	42.6	45
PEB1(200)	PGF100	1.61 (82.8)	26.5	41.3	47
PEB1(200)	PGF200	1.27 (65.0)	20.8	40.5	39
PEB1(250)	$PANI^E$	0.16 (6.4)	2.3	26.2	40
PEB1(250)	PGF0	0.39 (15.3)	4.9	13.2	48
PEB1(250)	PGF50	0.70 (27.5)	8.8	18.1	51
PEB1(250)	PGF100	1.36 (53.1)	17	13.1	45
PEB1(250)	PGF200	1.12 (44.1)	14.1	17.6	43
PEB1PR(250)	ITO	0.08 (2.9)	0.7	18.8	55
PEB1PR(250)	$PANI^E$	0.24 (7.5)	2.4	35.6	60
PEB1PR(250)	PGF0	1.1 (34.7)	11.1	18.9	60
PEB1PR(250)	PGF50	1.92 (60.8)	17.1	17.5	64
PEB1PR(250)	PGF100	3.51 (109.8)	26.9	23.9	65
PEB1PR(250)	PGF200	2.10 (66.5)	18.7	22.2	62

[a]Capacitance measured by galvanostatic CD. All the measurements were done at a scan rate of 0.2 mA cm^{-2}. Electrolyte SPAn was injected between two electrodes to construct a sandwich-type ECCW.

S3. Supporting videos

Supporting Video 1. Color change of ECCW100 in a voltage range of 1.4/-2.0 V.

Supporting Video 2. Energy transfer from two ECCWs to a clock.

Supporting Video 3. Energy transfer from three ECCWs to an R-LED.

Supporting Video 4. Color change of a large area ECCW100 of 100 cm^2.

References

1. B. R. Koo, M. H. Jo, K. H. Kim and H. J. Ahn, *NPG Asia Mater.,* 2020, **12**, 10.
2. P. Yang, P. Sun, Z. Chai, L. Huang, X. Cai, S. Tan, J. Song and W. Mai, *Angew. Chem. Int. Ed.*, 2014, **53**, 11935-11939.
3. K. Zhou, H. Wang, J. Jiu, J. Liu, H. Yan and K. Suganuma, *Chem. Eng. J.*, 2018, **345**, 290-299.
4. J. Yan, T. Wei, B. Shao, Z. Fan, W. Qian, M. Zhang and F. Wei, *Carbon*, 2010, **48**, 487-493.
5. Q. e. Zhang, A. a. Zhou, J. Wang, J. Wu and H. Bai, *Energy Environ. Sci.*, 2017, **10**, 2372-2382.
6. A. VahidMohammadi, J. Moncada, H. Chen, E. Kayali, J. Orangi, C. A. Carrero and M. Beidaghi, *J. Mater. Chem. A*, 2018, **6**, 22123-22133.